Single-Molecule Magnets

DOI: 10.1002/anie.200804286

Enhancing the Quantum Properties of Manganese–Lanthanide Single-Molecule Magnets: Observation of Quantum Tunneling Steps in the Hysteresis Loops of a $\{Mn_{12}Gd\}$ Cluster**

*Theocharis C. Stamatatos, Simon J. Teat, Wolfgang Wernsdorfer, and George Christou**

Single-molecule magnets (SMMs) are individual molecules that function as single-domain nanoscale magnetic particles.[1,2] A SMM derives its properties from a combination of a high-spin ground state (S) and an easy axis type of magneto-anisotropy (negative zero-field splitting parameter, D), which results in a significant energy barrier to the reversal of the magnetization vector. Such species display both classical magnetization hysteresis, quantum tunneling of magnetization (QTM),[3] and quantum phase interference.[4] Thus, SMMs represent a molecular ("bottom-up") route to nanoscale magnetism,[5] with potential technological applications in information storage and spintronics at the molecular level,[6a] and use as quantum bits (qubits) in quantum computation[6b] by exploiting the QTM through the anisotropy barrier.[3,7] The upper limit to the barrier (U) is given by $S^2\,|\,D\,|$ or $(S^2\text{-}1/4)\,|\,D\,|$ for integer and half-integer S, respectively. In practice, QTM through upper regions of the barrier makes the true or the effective barrier (U_{eff}) lower than that of U.

Ideally, the QTM can be observed and studied in magnetization vs. DC (direct current) field hysteresis loops, appearing as distinct step-like features at periodic field values, at which levels on either side of the anisotropy barrier to relaxation are in resonance. The steps are thus field positions at which the magnetization relaxation rate increases owing to the onset of QTM. Such steps are a diagnostic signature of resonant QTM, and have been clearly seen only for a few classes of compounds, such as manganese, iron, and nickel SMMs.[3,4,7,8]

[*] Dr. T. C. Stamatatos, Prof. Dr. G. Christou
Department of Chemistry, University of Florida
Gainesville, FL 32611-7200 (USA)
Fax: (+1) 352-392-8757
E-mail: christou@chem.ufl.edu
Dr. S. J. Teat
Advanced Light Source, Lawrence Berkeley National Laboratory
1 Cyclotron Road, Mail Stop 2-400, Berkeley, CA 94720 (USA)
Dr. W. Wernsdorfer
Institut Laboratoire Louis Néel, CNRS & Università J. Fourier
BP-166, Grenoble, Cedex 9 (France)

[**] This work was supported by the U.S. National Science Foundation (Grant CHE-0414555 to GC). The Advanced Light Source is supported by the Director, Office of Science, Office of Basic Energy Sciences, of the US Department of Energy under Contract No. DE-AC02-05CH11231.

Supporting information for this article is available on the WWW under http://dx.doi.org/10.1002/anie.200804286.

The most fruitful source of SMMs is the manganese carboxylate chemistry. The prototype was the $[Mn_{12}O_{12}(O_2CR)_{16}(H_2O)_4]$ family,[2,4,9] and a number of others have since been discovered; almost all have been transition metal clusters, and the vast majority of them have been manganese clusters containing at least some manganese(III) ions. As the search for new SMMs expanded, several groups explored mixed transition metal/lanthanide (Ln) compounds, and particularly Mn–Ln ones, as an attractive area; these efforts were greatly stimulated by the Cu_2Tb_2 SMM reported by Matsumoto and co-workers.[10] The strategy is obviously to take advantage of the lanthanide ion's significant spin, and/or its large anisotropy, as reflected in a large D value, to generate SMMs distinctly different from the homometallic ones. Indeed, there are now several Mn–Ln SMMs, including $Mn_{11}Ln_4$,[11] $Mn_{11}Gd_2$,[12] Mn_5Ln_4,[13a] and Mn_6Dy_6[13b]. Many of them have exhibited magnetization hysteresis loops, but unfortunately none of them have displayed resolved QTM steps in these loops. Thus, the incorporation of lanthanide ions has led to a degradation of the quantum properties, as reflected in the QTM steps. The likeliest reason for the degradation of the quantum properties is the step broadening owing to the low-lying excited states resulting from very weak exchange interactions involving the 4f metal ion(s).

Herein we report a new structural type in mixed Mn–Ln SMMs having a $\{Mn_{12}Gd\}^{38+}$ core, in which clear QTM steps have been observed in the hysteresis loops of a mixed 3d–4f SMM for the first time. As a result, the D value of a 3d–4f SMM can be measured directly for the first time from the hysteresis data, that is, from magnetic field separation between the steps.

The reaction of $Mn(O_2CPh)_2$, nBu_4NMnO_4, $Gd(NO_3)_3$, and $PhCO_2H$ in a 4:1:4:32 molar ratio in nitromethane produced a dark brown solution, which upon filtration and slow evaporation of the solvent resulted in crystals of $[Mn_{12}GdO_9(O_2CPh)_{18}(O_2CH)(NO_3)(HO_2CPh)]$ (**1**) in 40% yield. The structure of **1**[14] consists of a $\{Mn^{II}Mn^{III}_{11}\}^{35+}$ cluster with a central Gd^{3+} ion (Figure 1). The $\{Mn_{12}Gd\}^{38+}$ core is held together by seven μ_4-O^{2-} and two μ_3-O^{2-} ions. Peripheral ligation is provided by a μ_4-, three μ_3-, fourteen μ-benzoate groups, a μ_3-formate group, a chelating NO_3^- on Mn12, and a terminal benzoic acid on Mn5. The formate probably comes from oxidation of nitromethane by the highly oxidizing MnO_4^- reagent. The metal oxidation states and the protonation levels of O^{2-} ions were established by bond valence sum (BVS) calculations[15] and the observation of manganese(III) Jahn–Teller (JT) elongation axes (Figure S1). All manganese atoms are six-coordinate, whereas the gadolinium

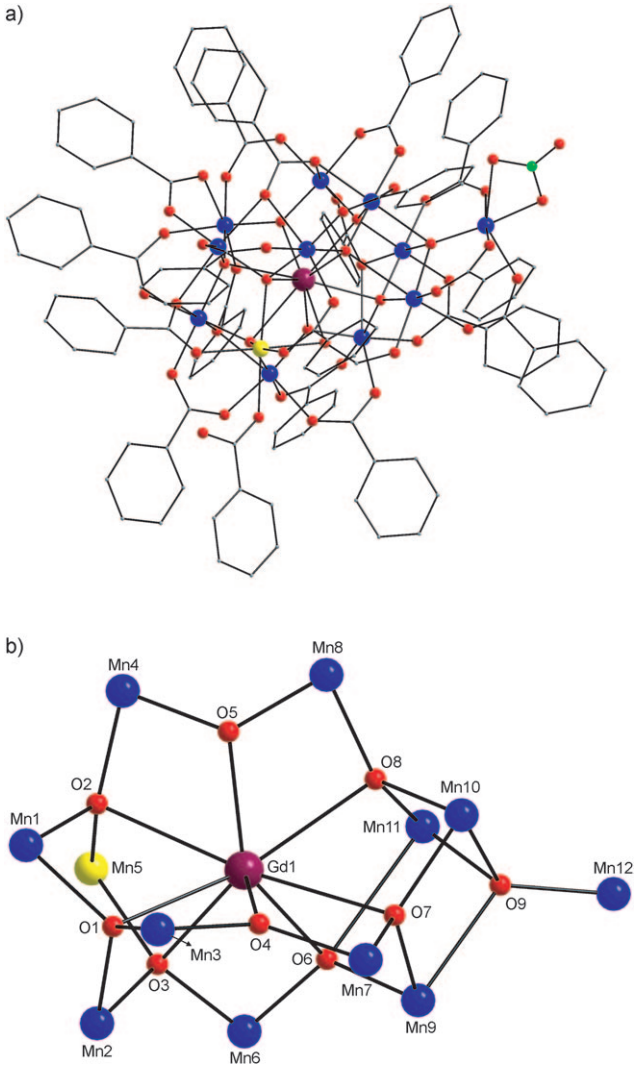

Figure 1. Molecular structure of a) **1** and b) its $\{GdMn_{12}O_9\}$ core. H atoms have been omitted for clarity. Gd purple, Mn(II) yellow, Mn(III) blue, O red, N green, C gray.

is nine-coordinate, being bound to eight O^{2-} ions and to the formate oxygen atom O201. In addition to the novel core topology, it is of great relevance to the magnetic properties to be described to note that **1** is the first Mn–Ln cluster to have a single lanthanide atom firmly encapsulated within a large manganese shell. Finally, there are no significant intermolecular interactions, only some very weak contacts involving C–H bonds.

Solid-state direct current (DC) magnetic susceptibility (χ_M) data were collected in the 5.0-300 K range in a 1 kOe (0.1 T) field (Supporting Information, Figure S2). The $\chi_M T$ value of 44.13 $cm^3 K mol^{-1}$ at 300 K decreases with decreasing temperature to 36.08 $cm^3 K mol^{-1}$ at 25.0 K and increases to 38.06 $cm^3 K mol^{-1}$ at 6.5 K, before dropping to 37.89 $cm^3 K mol^{-1}$ at 5.0 K. The latter decrease is assigned to Zeeman effects, zero-field splitting, and/or weak intermolecular interactions. The data therefore suggest that **1** has a significant ground state spin S value. To determine the ground state spin value S, magnetization (M) data were collected in the 0.1–5 T and 1.8–10.0 K ranges, and these are plotted as $M/N\mu_B$ versus H/T (Supporting Information, Figure S3). The data were fitted by matrix diagonalization to a model that assumes that only the ground state is populated. The model includes axial zero-field splitting ($D\hat{S}_z^2$) and the Zeeman interaction, and carries out a full powder average.[16] The best fit (solid lines in Figure S3) gave $S = 9$, $g = 2.00(3)$, and $D = -0.163(3)$ cm^{-1}, confirming a high ground-state spin with an appreciable magnetic anisotropy.

To investigate whether **1** might be a SMM, alternating current (AC) susceptibility measurements were carried out in a 3.5 Oe AC field oscillating at 5–1500 Hz, and with a zero DC field. Below circa 3.5 K, a frequency-dependent decrease in the in-phase ($\chi_M'T$) signal (Figure 2a), and a concomitant increase in the out-of-phase (χ_M'') signal (Figure 2b) were observed. Such χ_M'' signals suggest that the complex might be a SMM, but do not confirm that the complex is a SMM, as intermolecular interactions and phonon bottlenecks can have similar AC susceptibility responses.[17] Confirmation was therefore sought by magnetization versus DC field scans on single crystals of $\mathbf{1}\cdot 0.4MeNO_2\cdot 0.2H_2O$ using an array of micro-SQUIDs.[18] Magnetization hysteresis loops were observed below circa 0.7 K, at which point the coercivity increases with decreasing temperature (Figure 3) and increasing field sweep rate (Figure 4), as expected for an SMM below its blocking temperature (T_B). Complex **1** is thus a new SMM.

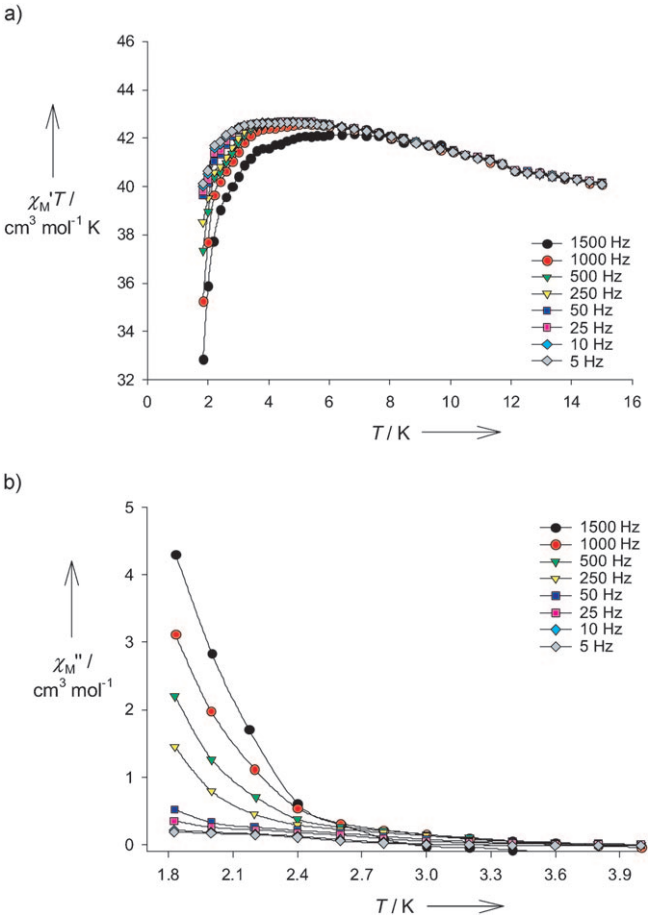

Figure 2. Plot of a) the in-phase (χ_M', as $\chi_M'T$) and b) out-of-phase (χ''_M) AC susceptibility signals for complex **1** measured in a 3.5 G field oscillating at the indicated frequencies.

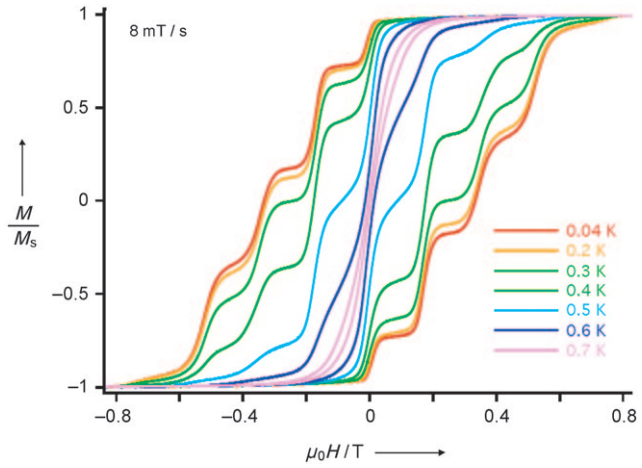

Figure 3. Magnetization *M* versus applied DC field *H* hysteresis loops for single crystals of **1**·0.4 $MeNO_2$·0.2 H_2O at the indicated temperatures. The magnetization is normalized to its saturation value M_s.

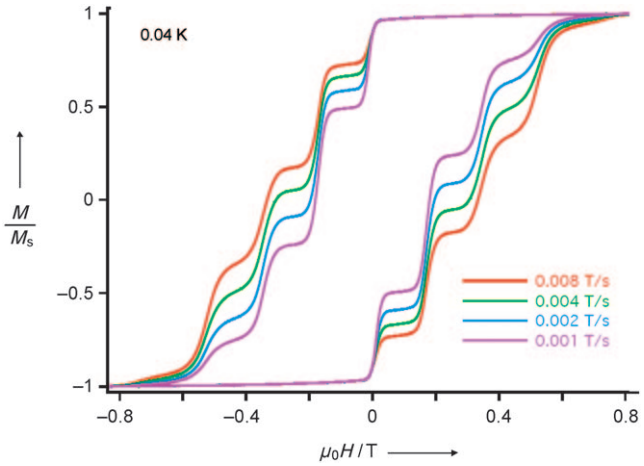

Figure 4. Magnetization *M* versus applied DC field *H* hysteresis loops for single crystals of **1**·0.4 $MeNO_2$·0.2 H_2O at the indicated field sweep rates. The magnetization is normalized to its saturation value M_s.

The surprising features in Figure 3 and 4 are the highly resolved QTM steps at periodic field positions. As stated earlier, such steps are diagnostic of resonant QTM,[3,4] and have been seen for several classes of SMMs in manganese,[8d,e,g,9] iron,[8a,c] and nickel[8b,h] compounds, with nuclearities up to Mn_{22}[8f] but usually M_{12} or below. They have also been seen in mononuclear lanthanide phthalocyanines.[19] In other words, they have never been seen before in mixed 3d–4f complexes. The first step in sweeping the field in Figure 3 and 4 from one saturating value to the other occurs at zero field, where the double-well potential energy curve is symmetric and M_s levels on one side of the barrier are in resonance with those on the other, allowing tunneling to occur through the barrier. Additional steps are then seen at periodic values of field when M_s levels are once again brought into resonance. The field separation between steps, ΔH, is proportional to D, as given by Equation (1), where k is the Boltzmann constant and μ_B is the Bohr magneton. The step positions in Figure 4 gave an average ΔH of 0.165 T and thus a $|D|/g$ value of

$$\Delta H = k|D|/g\mu_B \quad (1)$$

0.077 cm^{-1} (0.11 K). Assuming $g = 2.0$, this gives $|D| = 0.154\ cm^{-1}$ (0.22 K), in agreement with the value from the reduced magnetization fit for dried samples of **1**.

An Arrhenius plot was constructed using combined AC χ_M'' and DC magnetization decay versus time data. A fit of the thermally activated region to the Arrhenius relationship of Equation (2), where τ is the

$$\tau = \tau_0 \exp(U_{eff}/kT) \quad (2)$$

relaxation lifetime and τ_0 is the pre-exponential factor, gave $U_{eff} = 11.1\ cm^{-1}$ (16.0 K) and $\tau_0 = 2.4 \times 10^{-12}$ s (Supporting Information, Figure S4). The mean barrier U_{eff} is thus smaller than the calculated value $U = S^2|D| = 17.8$ K, as expected for QTM between higher energy M_s levels of the $S = 9$ manifold. Below circa 0.25 K, the relaxation becomes temperature-independent, indicating that the relaxation is now purely by ground state QTM directly between the lowest energy $M_s = \pm 9$ levels of the $S = 9$ manifold, and no longer via a thermally (phonon) assisted pathway involving higher-energy M_s levels.

The crucial question now is why complex **1** should show such clean quantum behavior with sharp, well-resolved QTM steps, whereas all previous Mn–Ln SMMs have not? This would be invaluable knowledge for continuing attempts to take advantage of the lanthanides in the SMM field. We believe that the single gadolinium atom in **1** is more strongly exchange–coupled to the Mn_x shell than is usually the case in Mn–Ln clusters as a result of the large number of O^{2-} (eight) ions bridging between gadolinium and manganese. As O^{2-} ions are good mediators of exchange interactions, the cumulative effect of eight of them should result in exchange coupling of the gadolinium to the Mn_x shell that is stronger than usual, albeit still weak in an absolute sense. Consequently, for the first time, the incorporation of lanthanide ions into a Mn_x cluster has not led to a high density of very low-lying excited states. This conclusion is supported by the $\chi_M'T$ versus T plot (Figure 2a), in which $\chi_M'T$ increases with decreasing T below 15 K as excited states with $S < 9$ are depopulated and reaches a plateau at about 5 K to a value of about 42.5 $cm^3\,K\,mol^{-1}$ that is consistent with an almost 100 % population of the $S = 9$ ground state. This observation clearly supports a relatively well-isolated ground state for this Mn–Ln cluster. All the previous Mn–Ln complexes have not shown such behavior, with one exception that contained Ln^{3+} ions bound to only a few O^{2-} ions, and/or have contained Ln–Ln interactions, which are known to be extremely weak. The Mn–Ln interaction, which was observed previously in the $Mn_{11}Gd_2$ complex,[12] had the following scenario: one Gd^{3+} ion was bridged to the manganese atoms by seven O^{2-} ions, and the other Gd^{3+} ion was bound to only one O^{2-} ion that led to low-lying excited states, although the former is more strongly exchange-coupled. We therefore conclude that it is necessary to have a large number of O^{2-} ions bridging the manganese to the lanthanide ion(s) in Mn–Ln clusters to observe enhanced quantum behavior as observed in **1**. Attempts to synthesize analogues of **1** are currently being pursued with various other anisotropic lanthanide ions to

probe changes to the quantum properties owing to the greater spin–orbit effects.

Experimental Section

1·0.4 $MeNO_2$·0.2 H_2O: Solid $PhCO_2H$ (2.00 g, 16.4 mmol) was dissolved in hot $MeNO_2$ (45 mL) with stirring, and the resulting colorless solution was treated with solid $Mn(O_2CPh)_2$·2 H_2O (0.70 g, 2.1 mmol) and $Gd(NO_3)_3$·6 H_2O (1.14 g, 2.1 mmol), which caused a rapid change of color from colorless to dark red. The solution was stirred at 80 °C for 10 min, and during this period solid nBu_4NMnO_4 (0.19 g, 0.53 mmol) was added in small portions. The resulting dark brown slurry was filtered, and the filtrate was left undisturbed to concentrate slowly by evaporation. After five days, X-ray quality dark-brown plate-like crystals of **1**·0.4 $MeNO_2$·0.2 H_2O had formed, and were collected by filtration, washed with $MeNO_2$ (2 × 5 mL) and Et_2O (3 × 5 mL), and dried under vacuum. Yield: 40 %. Elemental analysis (%) calcd for $C_{134}H_{97}Mn_{12}GdNO_{52}$ (**1**): C 47.76, H 2.90, N 0.42; found: C 47.69, H 3.06, N 0.37. Selected IR data (KBr pellets): $\tilde{\nu}$ = 3399 (mb), 3063 (m), 1693 (m), 1672 (m), 1597 (vs), 1535 (vs), 1494 (m), 1417 (sb), 1309 (m), 1271 (m), 1177 (m), 1158 (m), 1069 (m), 1025 (m), 1000 (w), 937 (w), 841 (w), 778 (w), 715 (s), 683 (m), 638 (m), 570 (mb), 513 (w), 442 (w), 424 (w) cm^{-1}.

Caution! Permanganate (MnO_4^-) salts are potentially explosive and should be synthesized and used in small quantities, and treated with utmost care at all times.

Received: August 29, 2008

Keywords: cluster compounds · lanthanides · magnetic properties · manganese · single-molecule magnets

[1] a) O. Kahn, *Molecular Magnetism*, VCH Publishers, New York, **1993**; b) D. Gatteschi, *Adv. Mater.* **1994**, *6*, 635 – 645.

[2] a) R. Sessoli, D. Gatteschi, D. N. Hendrickson, G. Christou, *MRS Bull.* **2000**, *25*, 66 – 71; b) R. Sessoli, H.-L. Tsai, A. R. Schake, S. Wang, J. B. Vincent, K. Folting, D. Gatteschi, G. Christou, D. N. Hendrickson, *J. Am. Chem. Soc.* **1993**, *115*, 1804 – 1816; c) R. Sessoli, D. Gatteschi, A. Caneschi, M. A. Novak, *Nature* **1993**, *365*, 141 – 143.

[3] a) J. R. Friedman, M. P. Sarachik, J. Tejada, R. Ziolo, *Phys. Rev. Lett.* **1996**, *76*, 3830 – 3833; b) L. Thomas, L. Lionti, R. Ballou, D. Gatteschi, R. Sessoli, B. Barbara, *Nature* **1996**, *383*, 145 – 147; c) S. M. J. Aubin, N. R. Gilley, L. Pardi, J. Krzystek, M. W. Wemple, L.-C. Brunel, M. B. Maple, G. Christou, D. N. Hendrickson, *J. Am. Chem. Soc.* **1998**, *120*, 4991 – 5004; d) B. Barbara, W. Wernsdorfer, L. C. Sampaio, J. G. Park, C. Paulsen, M. A. Novak, R. Ferrer, D. Mailly, R. Sessoli, A. Caneschi, K. Hasselbach, A. Benoit, L. Thomas, *Magn. Magn. Mater.* **1995**, *140*, 1825 – 1828.

[4] a) W. Wernsdorfer, R. Sessoli, *Science* **1999**, *284*, 133 – 135; b) W. Wernsdorfer, M. Soler, G. Christou, D. N. Hendrickson, *J. Appl. Phys.* **2002**, *91*, 7164 – 7166; c) W. Wernsdorfer, N. E. Chakov, G. Christou, *Phys. Rev. Lett.* **2005**, *95*, 037203.

[5] a) G. Christou, *Polyhedron* **2005**, *24*, 2065 – 2075; b) E. K. Brechin, *Chem. Commun.* **2005**, 5141 – 5153.

[6] a) L. Bogani, W. Wernsdorfer, *Nat. Mater.* **2008**, *7*, 179 – 186; b) M. N. Leuenberger, D. Loss, *Nature* **2001**, *410*, 789 – 793.

[7] M. N. Leuenberger, F. Meier, D. Loss, *Monatsh. Chem.* **2003**, *134*, 217 – 233.

[8] a) D. Gatteschi, R. Sessoli, *Angew. Chem.* **2003**, *115*, 278 – 309; *Angew. Chem. Int. Ed.* **2003**, *42*, 268 – 297; b) M. N. Leuenberger, E. M. Mucciolo, *Phys. Rev. Lett.* **2006**, *97*, 126601 – 126604; c) W. Wernsdorfer, A. Caneschi, R. Sessoli, D. Gatteschi, A. Cornia, V. Villar, C. Paulsen, *Phys. Rev. Lett.* **2000**, *84*, 2965 – 2968, and references therein; d) G. Aromi, S. Bhaduri, P. Artús, K. Folting, G. Christou, *Inorg. Chem.* **2002**, *41*, 805 – 817; e) T. C. Stamatatos, D. Foguet-Albiol, S.-C. Lee, C. C. Stoumpos, C. P. Raptopoulou, A. Terzis, W. Wernsdorfer, S. O. Hill, S. P. Perlepes, G. Christou, *J. Am. Chem. Soc.* **2007**, *129*, 9484 – 9499; f) J. T. Brockman, T. C. Stamatatos, W. Wernsdorfer, K. A. Abboud, G. Christou, *Inorg. Chem.* **2007**, *46*, 9160 – 9171; g) G. Rajaraman, M. Murugesu, E. C. Sanudo, M. Soler, W. Wernsdorfer, M. Helliwell, C. Muryn, J. Raftery, S. J. Teat, G. Christou, E. K. Brechin, *J. Am. Chem. Soc.* **2004**, *126*, 15445 – 15457; h) E.-C. Yang, W. Wernsdorfer, S. Hill, R. S. Edwards, M. Nakano, S. Maccagnano, L. N. Zakharov, A. L. Rheingold, G. Christou, D. N. Hendrickson, *Polyhedron* **2003**, *22*, 1727 – 1733.

[9] For some representative examples, see: a) H.-J. Eppley, H.-L. Tsai, N. de Vries, K. Folting, G. Christou, D. N. Hendrickson, *J. Am. Chem. Soc.* **1995**, *117*, 301 – 317; b) N. E. Chakov, M. Soler, W. Wernsdorfer, K. A. Abboud, G. Christou, *Inorg. Chem.* **2005**, *44*, 5304 – 5321; c) S. M. J. Aubin, Z. Sun, L. Pardi, J. Krzystek, K. Folting, L.-C. Brunel, A. L. Rheingold, G. Christou, D. N. Hendrickson, *Inorg. Chem.* **1999**, *38*, 5329 – 5340; d) N. E. Chakov, J. Lawrence, A. G. Harter, S. O. Hill, N. S. Dalal, W. Wernsdorfer, K. A. Abboud, G. Christou, *J. Am. Chem. Soc.* **2006**, *128*, 6975 – 6989.

[10] S. Osa, T. Kido, N. Matsumoto, N. Re, A. Pochaba, J. Mrozinski, *J. Am. Chem. Soc.* **2004**, *126*, 420 – 421.

[11] A. Mishra, W. Wernsdorfer, K. A. Abboud, G. Christou, *J. Am. Chem. Soc.* **2004**, *126*, 15648 – 15649.

[12] V. M. Mereacre, A. M. Ako, R. Clerac, W. Wernsdorfer, G. Filoti, J. Bartolome, C. E. Anson, A. K. Powell, *J. Am. Chem. Soc.* **2007**, *129*, 9248 – 9249.

[13] a) V. Mereacre, A. M. Ako, R. Clerac, W. Wernsdorfer, I. J. Hewitt, C. E. Anson, A. K. Powell, *Chem. Eur. J.* **2008**, *14*, 3577 – 3584; b) C. M. Zaleski, E. C. Depperman, J. W. Kampf, M. L. Kirk, V. L. Pecoraro, *Angew. Chem.* **2004**, *116*, 4002 – 4004; *Angew. Chem. Int. Ed.* **2004**, *43*, 3912 – 3914.

[14] a) Crystal structure data for **1**·0.4 $MeNO_2$·0.2 H_2O: $C_{134.40}H_{98.60}Mn_{12}GdN_{1.40}O_{52.75}$, M_r = 3393.68, monoclinic, space group $P2_1/c$, a = 18.2095(7), b = 22.5820(8), c = 32.5705(12) Å, β = 97.792(2)°, V = 13269.6(8) Å^3, Z = 4, ρ_{calcd} = 1.699 g cm^{-3}, T = 150(2) K, 156349 reflections collected, 33173 unique (R_{int} = 0.0534), $R1$ = 0.0406 and $wR2$ = 0.1057 using 23696 reflections with $F^2 > 2\sigma$. The asymmetric unit contains the complete {$Mn_{12}Gd$} cluster and 0.4 $MeNO_2$ and 0.2 H_2O molecules of crystallization. All non-hydrogen atoms were refined anisotropically except for the partial solvent molecules. Hydrogen atoms were placed geometrically on the phenyl groups and the formate. All H atoms were constrained and refined using a riding model. The H atoms on the $MeNO_2$ could neither be found in the difference map nor placed geometrically, and were therefore omitted from the refinement; b) CCDC 694302 contains the supplementary crystallographic data for this paper. These data can be obtained free of charge from The Cambridge Crystallographic Data Centre via www.ccdc.cam.ac.uk/data_request/cif..

[15] a) Bond-valence sum (BVS) calculations for the manganese and selected oxygen atoms of **1** gave values of 1.96 for the Mn^{2+} ion, 2.76–3.07 for Mn^{3+} ions, and 1.77–2.01 for O^{2-}; b) W. Liu, H. H. Thorp, *Inorg. Chem.* **1993**, *32*, 4102 – 4105; c) I. D. Brown, D. Altermatt, *Acta Crystallogr. Sect. B* **1985**, *41*, 244 – 247.

[16] MAGNET, E. R. Davidson, Indiana University.

[17] N. E. Chakov, W. Wernsdorfer, K. A. Abboud, G. Christou, *Inorg. Chem.* **2004**, *43*, 5919 – 5930, and references therein.

[18] W. Wernsdorfer, *Adv. Chem. Phys.* **2001**, *118*, 99 – 192.

[19] N. Ishikawa, M. Sugita, W. Wernsdorfer, *J. Am. Chem. Soc.* **2005**, *127*, 3650 – 3651.

